COMPARISON OF TRACKING SIMULATION WITH EXPERIMENT ON THE GSI UNILAC

X.Yin[1,2], L. Groening[2], I. Hofmann[2], W. Bayer[2], W. Barth[2]， S.Richter[2],
S. Yaramishev[2], A. Franchi[3], A. Sauer[4]
[1]*Institute of Modern Physics, Chinese Academy of Sciences, 730000, Lanzhou, China*
[2]*GSI Darmstadt, Planckstrasse 1, 64291 Darmstadt, Germany*
[3]*Accelerator Beam Physics Group, CERN. Switzerland*
[4]*IAP Frankfurt University, Frankfurt,Germany*

Abstract

In the European framework 'High Intensity Pulsed Proton Injector' (HIPPI), the 3D linac code comparison and benchmarking program with experiment have been implemented. HALODYN and PARMILA are two of the codes involved in this work. In this paper, the phase space distributions of the Alvarez DTL section are compared with the obtained distribution from experiment results which were carried out on the GSI UNILAC. Between the predictions from two codes, these results show some agreement comparing with the experiment results for low current case. And the physics aspects of the different linac design and beam dynamics simulation codes are also discussed.

1. INTRODUCTION

The main tasks of beam dynamics work package of 'HIPPI' project are the validation and benchmarking of 3D linac codes. Some comparison works have been performed [1]. In the overview paper [2, 3] the comparison step and tracking simulation were described based on the UNILAC Alvarez DTL.

Another important task, "Tracking Vs Experimental", is to find the tracking simulation how much agreement with measurement results both at the entrance and exit of the DTL and analysis the code validation based on the simulation results and experiment. As part of our effort to compare the beam simulation results from different codes, the 3D PIC tracking simulations have been performed with HALODYN and PARMILA based on the beam experiments which were proposed at GSI, assuming an initial 6D Gaussian distribution at the measurement point where is the beam entrance of the DTL.

2. CODES

The HALODYN code [4] has been written by the Department of Physics at the University of Bolognaand is a Particle-In-Cell code. The main feature of this code is the space-charge field can be computed by a micromap approach on a 3D spatial grid at each time step by using the Vlasov model. The Poisson solver is based on a 3D FFT. In the DTL sections, the transport elements are described by a sequence of drift, quadrupole and thin-lens RF cavities, whose accelerating voltage is inferred from the averaged accelerating electric fields. In our calculation, the grid resolution of HALODYN codes is of $2^5 \times 2^{11}$ for HALODYN.

PARMILA is a scalar code developed in Los Alamos (LANL) [5]. The user can choose either a 2D *r-z* (SCHEFF) or a 3D (PICNIC) PIC Poisson solver with open boundary conditions. The DTL structure has been defined by using the "DTL" command line. The RF is modelled making use of either the Transit-Time-Factor (TTF) table generated by SUPERFISH or a nonlinear thin kick. This code computes the space-charge forces by assuming an elliptical cylindrical symmetry

of the beam bunch. Each particle behaves as a ring of charge that contributes to the electric field on a two-dimensional (r, z) mesh. The number of intervals in each dimension of the space-charge mesh is fixed at a user-defined setting for an entire beam-dynamics run. In our calculation, the initial mesh intervals in the radial ΔR_{SC} and longitudinal directions ΔZ_{SC} are both 0.05cm, and the number of mesh intervals in these directions N_R, N_Z are 20 and 40 respectively.

Additionally HALODYN code has been developed under the UNIX environments system, PARMILA runs in the Windows platform. In the simulation, 5000 macroparticles are employed in HALODYN, while 100000 in PARMILA. More details of the individual codes can be found in the references cited above.

It should be mentioned that the PARMILA code was although developed for ion beam originally. When it was used to simulate for ion Z>1, we found that the beam current parameter should be multiply a factor using the following equation.

$$I = \frac{I_{eff}}{\eta} \times m \qquad (1)$$

where I is the beam current parameter used in PARMILA code in mA, I_{eff} is the effective current which is the real beam current in RF cavity, $\eta = 8.5$ is the mass-to-charge ratio for $^{238}U^{28+}$, m is the mass of the ion which is simulated in PARMILA. For example, when the I_{eff} is 37.5mA which is the operating beam current in the GSI UNILAC, the simulation current of Proton, $^{40}Ar^{10+}$ and $^{238}U^{28+}$ are 4.411mA, 176.44mA and 1050mA, respectively. Figure1shows the simulation results for different ions in the code benchmarking task using PARMILA and HALODYN [2]. As shown in Figure 1(a), the simulation results get excellent agreement for three kinds of particle in PARMILA. And Figure1(b) shows the benchmarking results for these two codes in case 2 which is the second type initial distribution in the simulation [3]. Basically the results of two codes also get excellent agreement. It demonstrates that the modification of current parameter in PARMILA what we have done is correct.

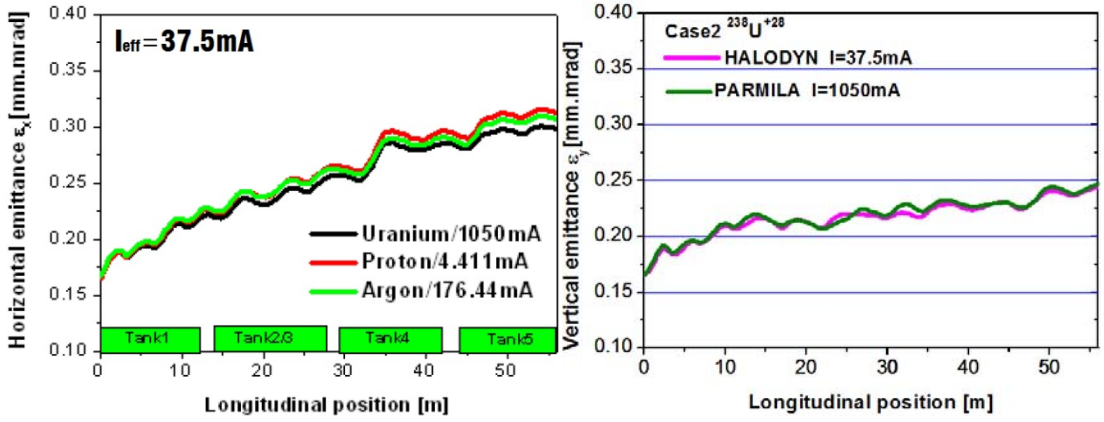

(a) (b)

Figure1.Code benchmarking simulation for PARMILA and HALODYN

3. EXPERIMENT SET-UP

The GSI UNILAC [6] was designed to accelerate all ion species with mass over charge ratios of up to 8.5 and to fill the heavy ion synchrotron SIS up to its space charge limit. Fig.2 shows the schematic overview of the UNILAC. The main part of the UNILAC consists of the High Current Injector (HSI), a gas stripper and the Alvarez DTL. The HIS is comprised by a RFQ and two IH-structures injector operated at 36 MHz, which will accelerate the particles to 1.4 MeV/u. And then the Alvarez DTL (108 MHz) will accelerate the particles to 11.4 MeV/u .

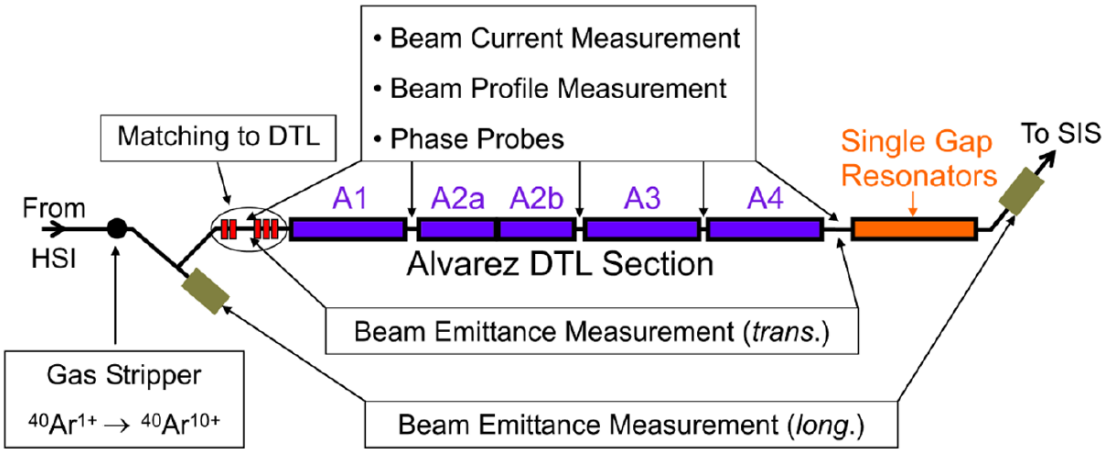

Figure2. Schematic overview of the GSI UNILAC.

Measurements of transverse phase space distributions were performed before and after the Alvarez accelerator with a periodic focusing channel [7], respectively. The set-up of the experiment is also shown in Fig1. Both transverse planes were measured simultaneously. The five quadrupole lenses before the DTL were set in order to maximize the beam transmission. All the presented measurements were carried out with $^{40}Ar^{+10}$ beam at 3uA.

4. EXPERIMENTAL RESULTS

As part of HIPPI-Beam Dynamics work package duty, we carried out beam experiment with $^{40}Ar^{+10}$ beam at 3uA choosing to start with the UNILAC Alvarez DTL tanks ($\beta = 0.054638 - 0.155$). Fig.3 shows the transverse phase-space distributions obtained in the measurement with a slit-grid device before Alvarez DTL. The measured values, 9.70mm-mrad and 7.91mm-mrad, are 90% of unnormalized emittances in the horizontal and vertical planes, respectively. For the simulation reason, they must be converted into normalized total emittances. Thus one can get the total normalized uniform RMS emittance 0.133mm-mrad and 0.108mm-mrad in the horizontal and vertical planes with $\beta = 0.054638$.

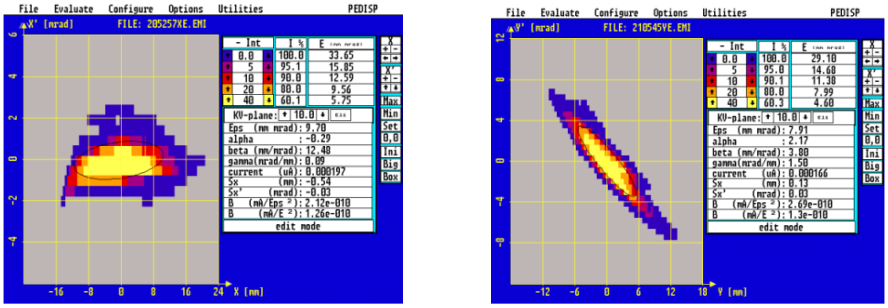

Figure3. Measured horizontal (left) and vertical (right) phase-space distribution before Alvarez DTL.

Fig.4 shows the obtained emittances after the Alvarez DTL where is the beam exit. The emittance were 4.5 mm-mrad and 2.83 mm-mrad of unnormalized emittances in the horizontal and vertical planes, respectively.

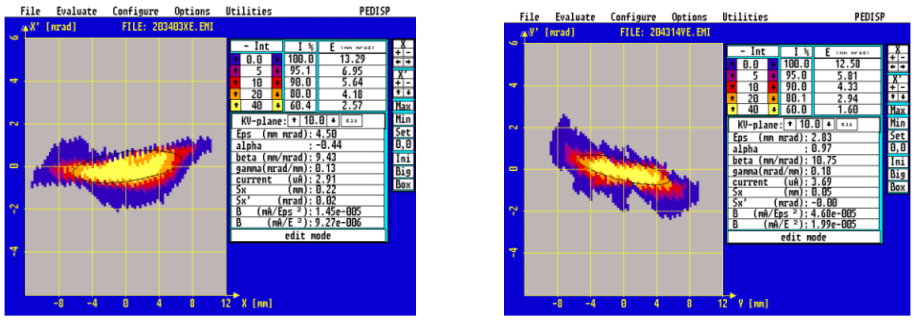

Figure4. Measured horizontal (left) and vertical (right) phase-space distribution after Alvarez DTL.

5. COMPARISON OF TRACKING SIMULATION WITH EXPERIMENT

In the tracking simulations, the Twiss parameters were obtained from the experiment results in low current. The input distribution is as usual a 6D-Gaussian (truncated in each phase space at 3σ), representing a $^{40}Ar^{+10}$ beam of kinetic energy W=1.396 MeV/u. Other beam and lattice parameters are listed in Tab.1.

Table1: Initial distribution parameters

	x-x'	y-y'	z-z'
α	-0.29	2.17	-0.15
β[cm/rad]	12.48E+2	3.80E+2	2.75784E+2
γ[rad/cm]	0.09E-2	1.05E-2	0.37E-2
$\varepsilon_{q\ u,t}$[cm-rad]	2.1825E-3	1.7798E-3	0.577338E-2

Fig.5 shows the initial distributions in the transverse phase spaces, which were calculated based on the measurement. As can be seen, the simulations results of both codes reproduce the measurement results exactly both in horizontal plane and vertical plane as shown in Fig3.

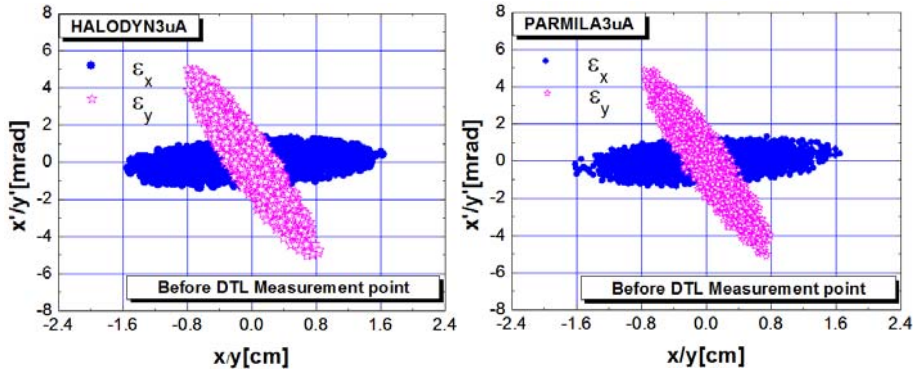

Figure5. Calculated horizontal (dot) and vertical (star) phase-space distribution before Alvarez DTL

Fig.6 shows the final distributions in the transverse phase-spaces at the exit of DTL. As can be found, the simulations results of both codes are basically agreement with experiment as shown in Fig 4. Furthermore, we can observe that a little discrepancy occurs between two codes. The simulation results of PARMILA are much more agreement with the experiment measurement than those of HALODYN. But we cannot conclude that HALODYN has no sufficient accuracy. It depends on the numerical algorithms which were applied in both codes.

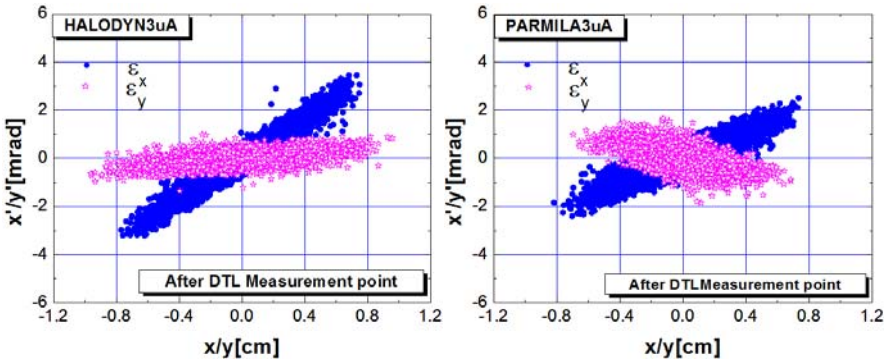

Figure6. Calculated horizontal (dot) and vertical (star)
phase-space distribution after Alvarez DTL.

Figure 7 shows the evolution of transverse emittance along the DTL section. It can be found that there is no obvious emittance growth under low current case. These results were demonstrated by the experiment.

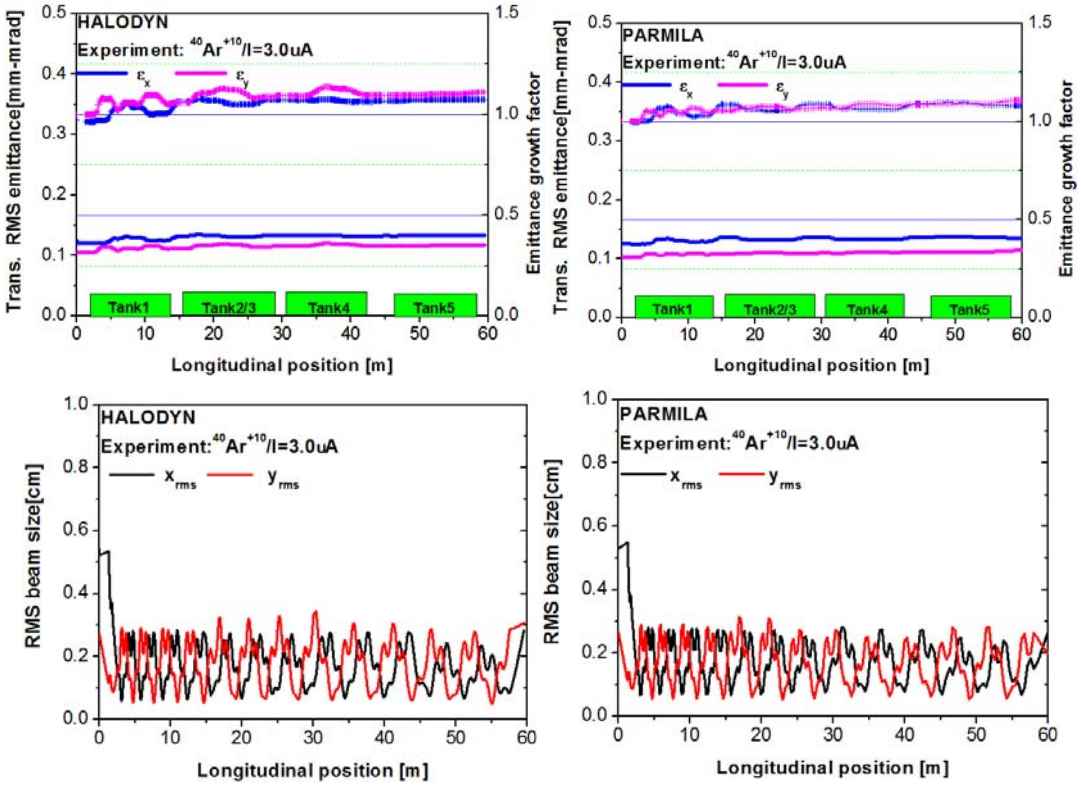

Figure7. The evolution of the transverse emittance and envelope along the Alvarez DTL.

Fig.8 shows the measured longitudinal phase-space distributions before DTL using the non-intersecting device. Fig.9 shows the calculated longitudinal phase-space distributions before and after DTL. Because there are some reasons to make the measure values be larger by about some factor in comparison to simulationin longitudinal phase [8]. Thus we assumed that initial longitudinal emittance parameters is some factor with measured one and tried to choose suitable one on longitudinal emittance. Comparing with experiment as shown, the initial distributions calculated by both codes are also compatible.

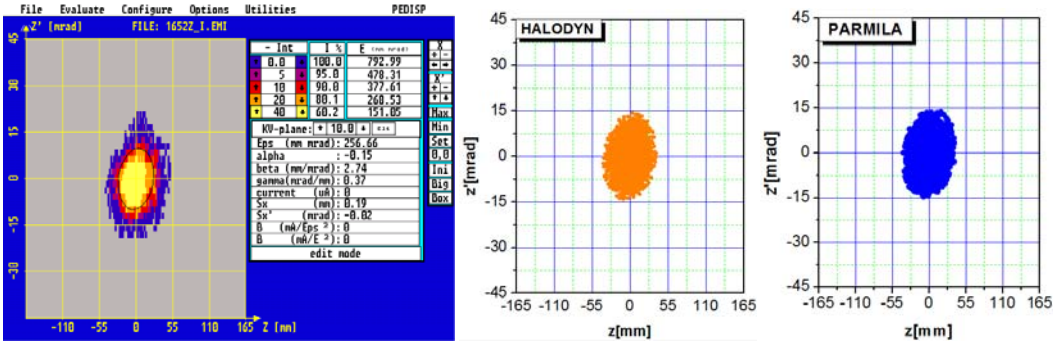

Figure8. Measured and calculated longitudinal phase-spaces distributions before Alvarez DTL.

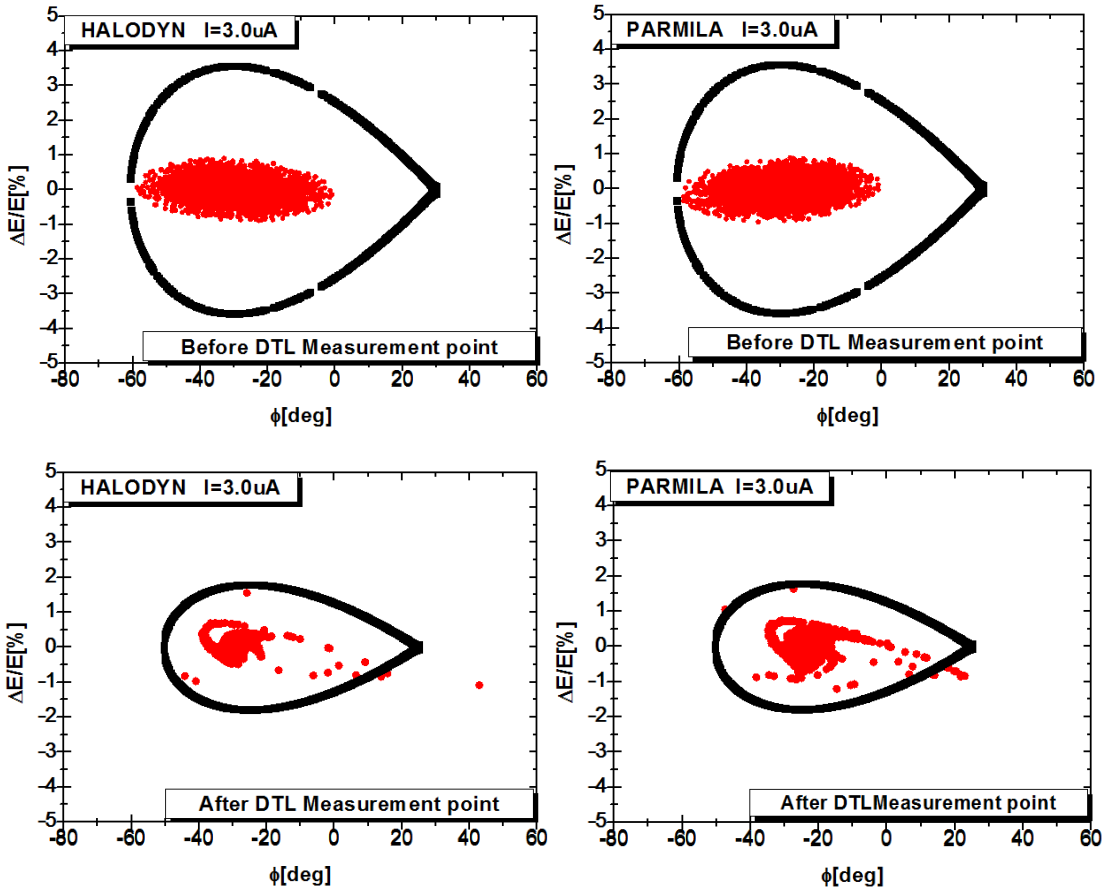

Figure9. Calculated longitudinal phase space ($\phi - \Delta E / E$)

distribution before (top) and after (bottom) Alvarez DTL

The measured and calculated rms emittance and growth ratios were summarized in Tab.2. Basically the both codes get excellent agreement in terms of the transverse RMS emittances. This demonstrates that codes with the 3D FFT in HALODYN and 2D Poisson solver SCHEFF in PARMILA are well within these values, confirming the robustness of the r-z approximations for the beam parameters under consideration. Furthermore, the calculate results are little small comparing with experiment results. This is acceptable in principle. But the emittance growth factors in vertical plane are larger than that of horizontal plane in both codes. This is reverse in the measurement.

Table2.The measured and calculated emittance and growth ratios

	Before DTL (hor./ver./lon.)	After DTL (hor./ver./lon.)	Emittance growth factor(hor./ver./lon.)
$\beta\gamma$	0.05472	0.1569	
Experiment[mm;mrad] (Uni, u,t)	9.7/7.91/256.6	4.5/2.83	
Experiment[mm;mrad] (Uni, rms,n)	0.133/0.108/0.351	0.177/0.111	1.34/1.028
HALODYN[mm;mrad](Gau ,rms,n)	0.125/0.106/0.333	0.134/0.117/0.663	1.07/1.11/1.99
PARMILA[mm;mrad](Gau ,rms,n)	0.125/0.103/0.333	0.135/0.114/0.534	1.08/1.11/1.6

More peculiar interest is the behaviour of the longitudinal emittance, shown in Fig.10 together with the beam transmission through the Alvarez DTL section (up curve).

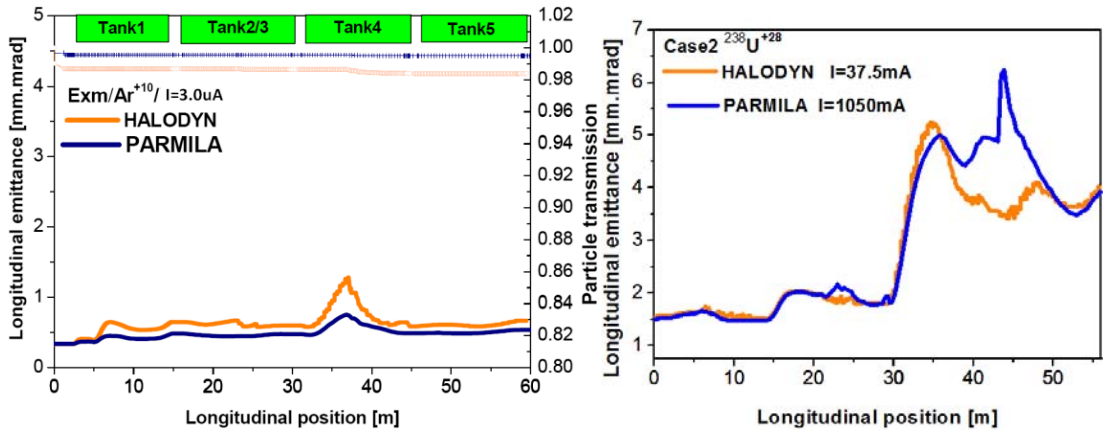

Figure10. Normalized longitudinal rms emittance computed by two codes along the DTL.

Fig.10 shows the longitudinal rms emittance calculated by two codes. Basically there are excellent agreements in the longitudinal plane in both codes before tank4, especially in the beginning drift section. A tiny increase of the emittance is observed due to the fact of the operation frequency jumping to 108 MHz at the entrance of the DTL. The obvious discrepancy occurs after the particles enter into the DTL because the different RF model were adopted in two codes as mentioned above. From Fig.10, we can also observe that the longitudinal emittance grow up from the entrance of tank4 predicted by both codes. It implied that a large dilution of the longitudinal phase space was accompanied to the emittance increase.It is believed that the peculiar and code-dependent behaviour after the first half of tank 4 is mainly driven by few particles close to the edge $|\Delta\varphi| \approx 180^0$.

It can be explained with the fact that the synchronous phase jumps from -30° to -25° when particles transport from tank3 to tank4.The bucket area shrinks at the same time. The longitudinal emittance experiences a weak growth due to the large bucket area in the first three thanks. When entering in tank 4, the phase jump accompanying the bucket area shrinks makes the bunch tails cross the separatrix, leading eventually to an even larger phase space dilution, as shown in Fig.10.Calculating results show that inserting a new buncher between tank3 and tank4 is an effective method to decrease the longitudinal emittance growth.

In Fig.10 it also shows how much degree the longitudinal RMS emittances can be depended on the particle loss definition (up curve). HALODYN will cut-off particle whose phase comparing to the synchronous phase is $|\Delta\varphi| > 180^0$ in longitudinal plane. PARMILA cut-off particle whose

energy spread relative to the reference energy is larger than 3% at each end of tanks. As we can observe form Fig.10, the particle transmissions are 98.4% and 99.5% for HALODYN and PARMILA through the Alvarez DTL section respectively.

6 CONCLUSIONS

Using the measured results, the tracking simulations were performed with HALODYN and PARMILA codes. Between the predictions from two codes using different mathematic model, these results presented here show some agreement comparing with the experiment results for low current case. Because of some reasons, the compressor factor about longitudinal emittance for simulation is still under considered. Due to the lack of the longitudinal emittance after DTL, the emittance growth factor is not presented in this paper. However two codes get excellent agreement both in transverse and longitudinal plane. It leads to conclusion that no gross errors have been made in the physics or methods of the codes. Further studies on the comparison should be carried out in high current region. And these studies should be investigated further with other codes.

ACKNOWLEDGEMENT

The authors wish to thank Prof. Ingo Hofmann for frequent valuable discussions and the GSI UNILAC group in carrying out the experiment. We are also grateful to Dr.A.Franchi and Dr.A.Sauer for their continue support on HALODYN and PARMILA.

We acknowledge the support of the European Community-Research Infrastructure Activity under the “FP6” Structuring the European Research Area” program.

REFERENCE

[1] S.Nath,J.Qiang,R.Ryne,etc. *Comparison of Linac simulation codes,* in Proceedings of the Particle Accelerator Conference, 2002, p264

[2] A.Franchi, W.Bayer, G.Franchetti, L.Groening, I.Hofmann, A.Orzhekhovskaya, S.Yaramyshev, X.Yin *Linac code benchmarking for the UNILAC experiment*, Proceeding of Linac 2006

[3] X.Yin,W.Bayer,A.Franchi,I.Hofmann,etc, *Status of Code Benchmarking for HIPPI*, HIPPI annual meeting,FZJ,September 27-29,2006

[4] G. Turchetti et al., *Accuracy analysis of a spectral Poisson solver*, Nucl. Intr. & Meth. A, vol. 561 Issue 2 (2006), pp. 223-229.

[5] D.A.Swenson, and J.E.Stovall, *PARMILA*, Los Alamos national Laboratory internal Memorandum, MP-3-19,January 1968.

[6] S.Yaramishev, W. Barth, L. Dahl, L.Groening, A.Kolomiets, T.Tretyakova, *Development of the versatile multi-particle code DYNAMION*, NIM A588(2006) 90-94

[7] P. Forck, A.Peters, P.Strehl, *Beam diagnostic for the upgraded UNILAC at GSI*, Proceeding of 6th EPAC,Stockholm,Sweden,p.1500(1998)

[8] P. Forck, et al., *Measurement of the six dimensional Phase Space at te New GSI High Current Linac*, Proc. of LINAC2000, Monterey, USA, (2000).